

Experimental testing and constitutive modeling of the mechanical properties of the swine skin tissue

SYLWIA D. ŁAGAN, ANETA LIBER-KNEĆ*

Institute of Applied Mechanics, Cracow University of Technology, Cracow, Poland.

Purpose: The aim of the study was an estimation of the possibility of using hyperelastic material models to fit experimental data obtained in the tensile test for the swine skin tissue. **Methods:** The uniaxial tensile tests of samples taken from the abdomen and back of a pig was carried out. The mechanical properties of the skin such as the mean Young's modulus, the mean maximum stress and the mean maximum elongation were calculated. The experimental data have been used to identify the parameters in specific strain-energy functions given in seven constitutive models of hyperelastic materials: neo-Hookean, Mooney–Rivlin, Ogden, Yeoh, Martins, Humphrey and Veronda–Westmann. An analysis of errors in fitting of theoretical and experimental data was done. **Results:** Comparison of load–displacement curves for the back and abdomen regions of skin taken showed a different scope of both the mean maximum loading forces and the mean maximum elongation. Samples which have been prepared from the abdominal area had lower values of the mean maximum load compared to samples from the spine area. The reverse trend was observed during the analysis of the values of elongation. An analysis of the accuracy of model fitting to the experimental data showed that, the least accurate were the model of neo-Hookean, model of Mooney–Rivlin for the abdominal region and model of Veronda–Westmann for the spine region. **Conclusions:** An analysis of seven hyperelastic material models showed good correlations between the experimental and the theoretical data for five models.

Key words: hyperelastic material, soft tissue, tensile test, pig's skin, constitutive model

1. Introduction

A skin is the biggest organ of a body. It is a complex tissue composed of several layers: epidermis, dermis and hypodermis. In addition, depending on the area of the body and the research direction in relation to the so-called Langer lines, it has different physical parameters (e.g., thickness, hardness and elasticity) [2], [9]. Therefore, it is difficult to mathematically describe the skin, both in terms of the behavior of individual layers and as a whole organ. Understanding of the mechanical properties of the skin tissue is important and used in such fields as medicine, surgery or dermatology to predict the effects of surgical treatment [5]. The knowledge acquired in *in vivo* and *in vitro* experiments is also used in the engineering de-

sign of surgical instruments and medical robots [4], [19], and by forensics experts to evaluate the history of the damage formation, the nature of skin lesions due to mechanical trauma or traffic accidents [22]. The legal regulations and ethical reasons make obtaining human skin for experimental research difficult. Therefore, the material of animal origin is widely used as a substitute for qualitative and quantitative studies and modeling. A pig's skin is the most similar to a human skin due to the greatest compatibility of anatomical features, thickness and mechanical properties, thus it is the most often used as substitute in the biomechanical studies [11], [16], [25]. Also mice and rats [12], monkeys [13] and bovines [1] have been used in experimental investigations. The results of tests show that skin is an anisotropic, viscoelastic and non-linear material [2], [14], [25]. The visco-

* Corresponding author: Aneta Liber-Kneć, Institute of Applied Mechanics, Cracow University of Technology, al. Jana Pawła II 37, 31-864 Cracow, Poland. Tel: +48 692 586 152, e-mail: aliber@pk.edu.pl

Received: October 7th, 2016

Accepted for publication: December 5th, 2016

elastic properties of the skin are attributed to fluid impacts, in which the fiber network of collagen and elastin give the extensibility and flexibility of the tissue [15], [20]. The results of the study are also affected by the conditions of skin samples taken, e.g. the direction of samples taken [2], the origin of the sample (human, animal), gender, age [3], the conditions of storage including solution-medium, humidity-drying, temperature and time.

Based on the results of experimental studies of skin tissue subjected to different external loads (e.g., tension, compression) and strain rates [16], [18], constitutive modeling is possible. However, an application of constitutive models of hyperelastic materials requires simplifying the assumption describing the skin as an isotropic, non-linear elastic and incompressible material [10], [17]. Depending on the purpose of scientific research, constitutive modeling of biological tissues is used in many fields such as biomechanics of collisions, rehabilitation, tissue engineering, surgical simulations, drugs delivery systems [6], [24].

The aim of this study was an approximation of experimental results of the uniaxial tensile tests of the pig's skin tissue taken from different areas of the body (abdomen and spine region) with the use of selected hyperelastic material models. The existing hyperelastic models such as neo-Hookean, Mooney–Rivlin, Ogden, Yeoh, Martins, Humphrey and Veronda–Westmann were employed to estimate the accuracy of matching experimental and theoretical data as well as the evaluation of errors.

2. Materials and methods

Along the long axis, defined by the spine of a pig's body, two patches of skin tissue from the spine region and the abdomen of a domestic pig, which weighed ca. 130 kg, and was 8 months old, were taken. Hairs and the subcutaneous fat layer were removed from the skin. Then samples were cut in the perpendicular direction to the long axis of the pig's body. The length of the samples was 100.0 ± 0.1 mm, the width was 10.0 ± 0.1 mm and the thickness varied depending on the taken region. The thickness of the samples taken from the back was 2.3 ± 0.1 mm, and from the abdomen was 1.5 ± 0.1 mm. As prepared samples were packaged in a polypropylene foil and stored in a freezer at -18 °C. Before the experiment, samples were thawed at the temperature of 22 ± 2 °C in the period of 2 hours. The uniaxial tensile tests were performed on MTS

Insight 50 testing machine at the speed of 5 mm/min. The samples were mounted in the flat clamps with knurling cross. The initial length of samples was 50.0 ± 0.1 mm. Each set of samples contained a minimum of 5 samples.

Then, the appropriate procedures in order to obtain approximation of experimental data with mathematical record with the use of the software OriginPro7.5 were made. For each of the samples group (differing in the region of samples taken), the average experimental tensile curve was done and then recalculated to stress-strain curve. A typical stress–strain curve for the skin shows a nonlinear characteristics and consists of three phases. In the initial phase (I) of the load during the tensile test, the collagen fibers are woven in a diamond pattern, and large deformations of skin tissue appear at a relatively low load. This phenomenon is attributed to elastin fibers responsible for the stretching mechanism. The stress–strain curve is approximately linear in the first phase and a modulus of elasticity of the skin is low. Then the curve loses its linearity passing phase II. In the second phase the stiffness of the skin increases gradually, and collagen fibers are gradually straightened in the direction of the applied load. In phase III the stress–strain curve become linear again. Collagen fibers remain upright until the tensile strength of skin is achieved [2], [7].

According to the formula (1), the values of elastic modulus (E_I , E_{III}) for the two selected areas of deformation, corresponding to the small and large level of deformation (formulas (2)–(4)), were calculated. For each of the samples groups ranges of deformation had different values (see Fig. 1).

$$E_I = \frac{\delta\sigma^e}{\delta\varepsilon^e}, \quad E_{III} = \frac{\delta\sigma^k}{\delta\varepsilon^k}, \quad (1)$$

where $\delta\sigma^e$ – discrete increase of stress in phase I, $\delta\sigma^k$ – discrete increase of stress in phase III, $\delta\varepsilon^e$ – discrete increase of strain in phase I, $\delta\varepsilon^k$ – discrete increase of strain in phase III.

The constant cross section of the specimens during the tests was assumed. The average maximum stress σ_i (i – research group) was calculated using the measured tensile force F_i [N] and the average cross-section of the skin A_i [mm^2] by the formula (2):

$$\sigma_i = \frac{F_i}{A_i}. \quad (2)$$

Strain ε and stretch λ were calculated by the following formulas (3) and (4), where l_i [mm] is the length after elongation, l_0 is the initial length of the sample.

$$\varepsilon = \frac{\Delta l}{l_0} = \frac{l_i - l_0}{l_0}, \quad (3)$$

$$\lambda = \varepsilon + 1. \quad (4)$$

For such prepared input files, computational procedures associated with constitutive modeling of hyperelastic materials for the seven most popular models presented in the literature used for materials such as rubber, polymers and soft tissues, were made [17], [23]. Characteristics (curves) of the matching, the coefficient of determination R^2 (5) and the model constants C_i (in this paper $i = 1, 2, 3, 4$) corresponding to the material parameters were recorded. The formula for the coefficient of determination can be given as (5):

$$R^2 = \frac{\sum_{i=1}^n (\hat{y}_i - \bar{y})^2}{\sum_{i=1}^n (y_i - \bar{y})^2}, \quad (5)$$

where y_i is the real value of the experimental stress, \hat{y}_i is the theoretical value of the stress on the basis on models, \bar{y} is the arithmetic mean value of the experimental stress.

To evaluate the match between the theoretical $f_t(\lambda)$ and the experimental $f_e(\lambda)$ stretch function at each stretch level, the normalized error was calculated according to the formula (6) [32]:

$$ER(\lambda) = \frac{|f_e(\lambda) - f_t(\lambda)|}{f_e(\lambda)}. \quad (6)$$

To determine the values of C_i the algorithm of Levenberg–Marquardt (damped least-squares) was used.

A hyperelastic material models based on the definition of strain energy function, which is expressed in different ways, depend on the class or kind of materials considered. Assuming an isotropy of material, the strain-energy function (W) can be written as depended on the strain invariants of the deformation tensor of Cauchy–Green I_1, I_2, I_3 (7):

$$W_{\text{isotropic}} = W(I_1, I_2, I_3) \quad (7)$$

were:

$$I_1 = \lambda_1^2 + \lambda_2^2 + \lambda_3^2, \quad (8)$$

$$I_2 = \lambda_1^2 \lambda_2^2 + \lambda_2^2 \lambda_3^2 + \lambda_3^2 \lambda_1^2, \quad (9)$$

$$I_3 = \lambda_1^2 \lambda_2^2 \lambda_3^2 \quad (10)$$

and $\lambda_1, \lambda_2, \lambda_3$ – are the principal stretches.

Considering the conditions of the uniaxial tension of incompressible materials ($\sigma_2 = \sigma_3 = 0$) we get (11):

$$\lambda_1 = \lambda, \quad \lambda_2 = \lambda_3 = \frac{1}{\sqrt{\lambda}}. \quad (11)$$

Expressions of the left tensor invariant of deformations are also simplified and the deformation is brought to the primary stretches (12):

$$I_1 = \lambda^2 + 2 \frac{1}{\lambda}, \quad I_2 = 2\lambda + \frac{1}{\lambda^2}, \quad I_3 = 1. \quad (12)$$

The strain–energy function can be written in the form (13), where C_{ijk} are material constants:

$$W = \sum_{i+j+k=1}^{\infty} C_{ijk} (I_1 - 3)^i (I_2 - 3)^j (I_3 - 3)^k. \quad (13)$$

Soft tissue is an anisotropic material, so the standard models not exactly capture characteristics of these particularly materials. Both a new and difficult approach in tissues modeling is including information about an isotropic and anisotropic properties of material in the strain-energy function

For neo-Hookean material model the function of the strain energy density is written as the relationship of principal strains (14):

$$W = C_1(I_1 - 3). \quad (14)$$

In the case of the uniaxial tension, the Cauchy stress as a function of the strain invariants is given as (15):

$$\sigma = 2C_1 \left(\lambda^2 - \frac{1}{\lambda} \right). \quad (15)$$

In Mooney–Rivlin model the strain energy function is presented in the literature [17] as (16):

$$W = C_1(I_1 - 3) + C_2(I_2 - 3). \quad (16)$$

For uniaxial tension test the stresses can be expressed as (17):

$$\sigma = 2C_1 \left(\lambda^2 - \frac{1}{\lambda} \right) - 2C_2 \left(\frac{1}{\lambda^2} - \lambda \right). \quad (17)$$

The strain–energy function in Yeoh material model [17] is dependent on the first strain invariant (I_1) what can be written as (18):

$$W = C_1(I_1 - 3) + C_2(I_1 - 3)^2 + C_3(I_1 - 3)^3. \quad (18)$$

Using the invariant from Cauchy stress, the uniaxial stress can be obtained as (19):

$$\sigma = 2 \left(\lambda^2 - \frac{1}{\lambda} \right) \times \left(C_1 + 2C_2 \left(\lambda^2 + \frac{2}{\lambda} - 3 \right) + 3C_3 \left(\lambda^2 + \frac{2}{\lambda} - 3 \right)^2 \right). \quad (19)$$

The strain energy function in Ogden material model [1], [16], [21] depends on principal strain and was given as (20):

$$W = \frac{2\mu}{\alpha^2} (\lambda_1^\alpha + \lambda_2^\alpha + \lambda_1^{-\alpha} \lambda_2^{-\alpha} - 3). \quad (20)$$

And the stress was formulated as (21):

$$\sigma = \frac{2\mu}{\alpha^2} (\lambda^{\alpha-1} - \lambda^{-1(\alpha/2)}). \quad (21)$$

The formula of strain energy function proposed by Humphrey [17], which is a function of the components of the right Cauchy–Green tensor in an isotropic material, is written as (22):

$$W = C_1 (e^{C_2(I_1-3)} - 1). \quad (22)$$

In order to obtain the material parameters C_1 and C_2 , the stress formula given as (23) is used:

$$\sigma = 2 \left(\lambda^2 - \frac{1}{\lambda} \right) C_1 C_2 e^{C_2 \left(\lambda^2 + \frac{2}{\lambda} - 3 \right)} \quad (23)$$

Martins model [17] shows the strong influence of fibers stretch, and it was used for analysis of the skeletal muscles and formulated as (24):

$$W = C_1 (e^{C_2(I_1-3)} - 1) + C_3 (e^{C_4(\lambda-3)} - 1). \quad (24)$$

In the conditions of the uniaxial tension the stress is expressed as (25):

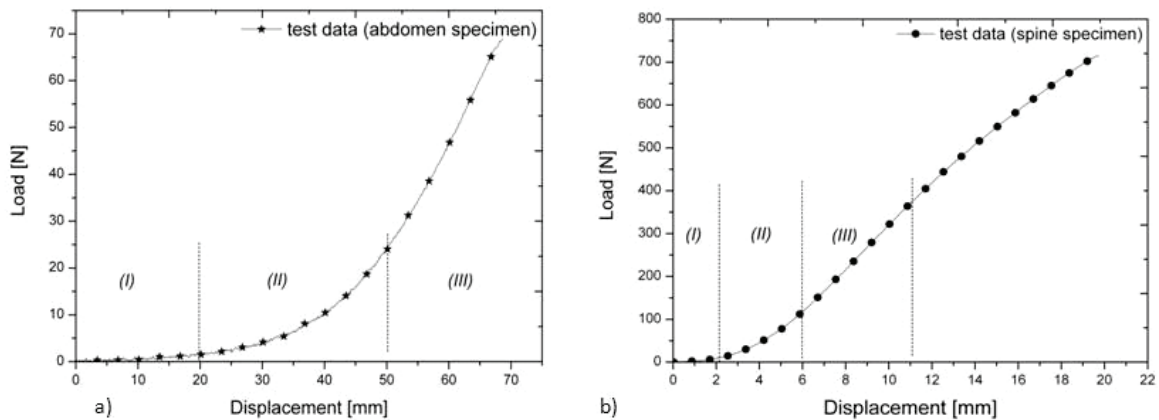


Fig. 1. The load–displacement curves for different regions of specimens taken: a) the abdomen region; b) the spine region

$$\sigma = 2 \left(\lambda^2 - \frac{1}{\lambda} \right) C_1 C_2 e^{C_2 \left(\lambda^2 + \frac{2}{\lambda} - 3 \right)} + 2\lambda(\lambda-1)C_3 C_4 e^{C_3(\lambda-1)^2}. \quad (25)$$

Veronda–Westmann [17] is the model of hyperelastic materials in which the strain energy function depends on principal strain invariants, and using the assumptions of an incompressible material can be written as (26):

$$W = C_1 (e^{C_2(I_1-3)} - 1) - \frac{C_1 C_2}{2} (I_2 - 3). \quad (26)$$

And the stress formula is given as

$$\sigma = 2 \left(\lambda^2 - \frac{1}{\lambda} \right) C_1 C_2 \left(e^{C_2 \left(\lambda^2 + \frac{2}{\lambda} - 3 \right)} - \frac{1}{2\lambda} \right). \quad (27)$$

3. Results

In both groups of specimens a typical stress–strain curve for the skin showed a nonlinear characteristics and consisted of three phases (Fig. 1). In Fig. 1, load–displacement curves for each of the research groups were presented. Comparing load–displacement curves for the spine and abdomen regions of the skin taken, a different scope of both the mean maximum loading forces and the mean maximum elongation were clearly visible (Fig. 2). Samples which have been prepared from the abdominal area had lower values of the mean maximum load compared to samples from the spine area (the abdominal area: 89.01 ± 11.75 N, the spine area: 772.48 ± 134.18 N). The reverse trend was observed during the analysis of the values of elongation. Samples from the abdomen region showed

significantly higher values of elongation ($\Delta l = 75.40 \pm 6.27$ mm) compared to the samples from the spine region ($\Delta l = 22.40 \pm 2.85$ mm).

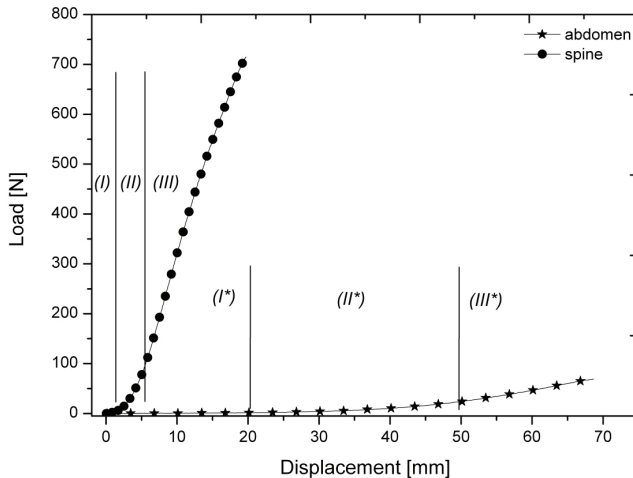


Fig. 2. The comparison of load–displacement curves for analyzed regions of specimens taken including area variation of Young's modulus (I*, II*, III*: the abdomen region, I, II, III: the spine region)

During the analysis of characteristics of the stress–strain (Fig. 3), similar relationship to described above can be observed. The value of average maximum stress calculated in relation to the average cross-section of samples was significantly different for the samples from different regions of taken. For the samples from the abdomen region this value was 6.09 ± 0.70 MPa compared to much higher value for samples from the spine region at 34.13 ± 6.27 MPa. In contrast, the mean maximum strain value reached 1.51 ± 0.1 for the abdominal samples and 0.46 ± 0.1 for samples from the back. The values of calculated Young's modulus for discrete areas (I) and (III) were summarized in Table 1.

Table 1. The summary of values of Young's modulus in phases (I) and (III) of stretching (\pm SD)

Young's modulus E [MPa]	abdomen region	spine region
E_I	0.41 ± 0.16	81.73 ± 15.04
E_{III}	7.55 ± 1.40	106.79 ± 13.62

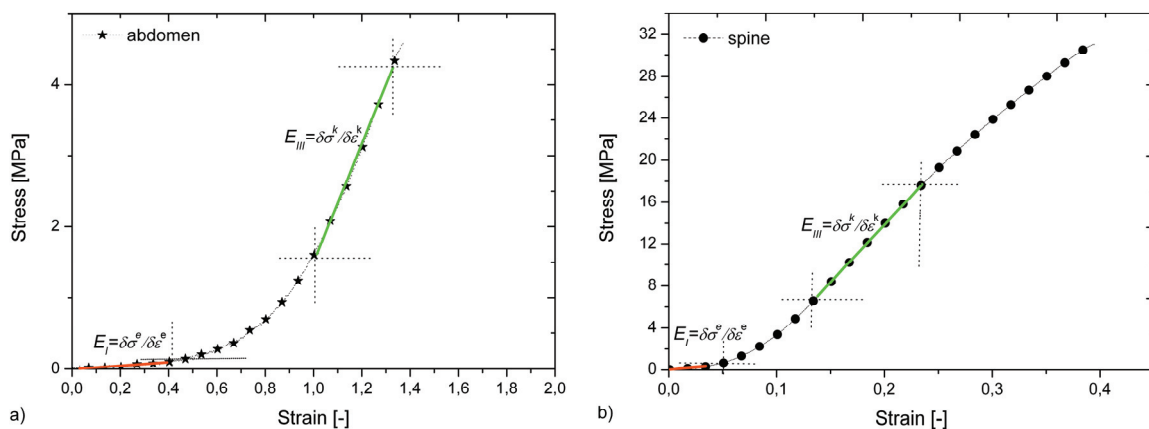


Fig. 3. The stress–strain characteristics with the selected linear range: a) samples taken from the abdomen; b) samples taken from the spine region

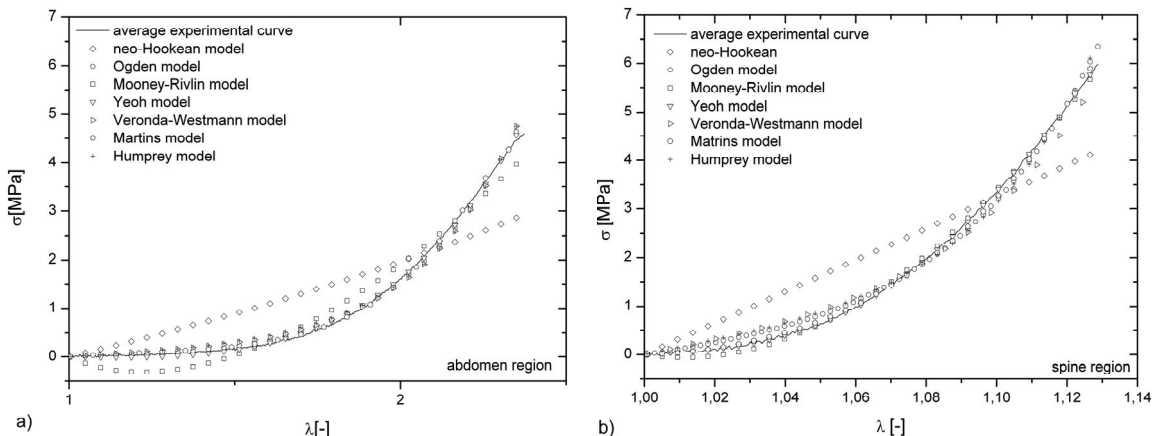


Fig. 4. The stress–stretch curves for skin samples including fitting of seven hyperelastic material models:
a) samples taken from the abdomen region; b) samples taken from the spine region

Table 2. The values of parameter C_i for constitutive hyperelastic material models calculated for experimental stress–stretch curves of pig's skin specimens

Material model	Place of the specimens taken			
	abdomen		spine	
	C_i	R^2	C_i	R^2
Neo-Hookean	0.281 ± 0.005	0.728	5.399 ± 0.127	0.805
Mooney–Rivlin	1.058 ± 0.014	0.961	80.498 ± 0.542	0.998
	-1.573 ± 0.028		-82.330 ± 0.594	
Ogden	0.057 ± 0.001	0.997	3.580 ± 0.073	0.993
	7.728 ± 0.028		27.413 ± 0.284	
Yeoh	-0.019 ± 0.002	0.998	0.687 ± 0.013	0.999
	0.052 ± 0.001		103.815 ± 0.567	
	0.003 ± 0.000		-400.051 ± 7.136	
Humphrey	0.130 ± 0.004	0.989	0.090 ± 0.004	0.988
	0.553 ± 0.006		26.824 ± 0.567	
Martins	0.873 ± 0.013	0.999	3.130 ± 2.272	0.998
	0.450 ± 0.056		-10.506 ± 5.120	
	1.407 ± 0.029		12.484 ± 3.218	
	-0.619 ± 0.087		7.984 ± 0.937	
Veronda–Westmann	0.466 ± 0.019	0.991	0.347 ± 0.025	0.979
	0.397 ± 0.006		15.008 ± 0.613	

The results of the tensile tests were used to verify the model fitting of the non-linear dependence of stress–stretch in the elastic range by the use of hyperelastic material models. The calculated material constants for implemented models were summarized in Table 2. The graphic presentation of models fitting for specimens from the abdomen and spine regions was shown in Fig. 4.

A summary of the material constants generated during the fitting procedure of seven selected constitutive models of hyperelastic materials to the experimental data and the values of coefficient of determination (R^2) were presented in Table 2. Depending on the model, the values of constants C_i were different. When the accuracy of the model fitting was compared to the experimental data, the least accurate were the model of neo-Hookean (<0.81), model of Mooney–Rivlin for the abdominal region (<0.97) and model of Veronda–Westmann for the spine region (<0.98). An analysis of the coefficient of determination was confirmed in observations of curves fitting. In Figure 4a) a good fitting was observed for five of the seven models throughout the whole range of stretch for samples from the abdomen. As showed in Figure 4b) better fitting was obtained for the second region of stress–stretch curve for samples from the back ($\lambda > 1.06$) for five of the seven models, and throughout the whole range of stretch for the models of Martins and Yeoh.

In Figs. 5 and 6, the error analysis for each material model for two regions of specimens taken was presented. For the abdomen region, a good correspondence agreement of the number of minima with the number of model constants C_i was observed. Such dependency was not observed for error curves for the skin from the spine region. The observed irregularities, which have occurred in the range of small deformations for the area of the back ($\lambda < 1.06$), confirmed the good match of hyperelastic material models for the pig's skin tissue from the back. Distinct differences in the variability of the error curves confirmed the heterogeneity of the tissue of the skin in relation to areas of the body.

4. Discussion

In several studies the mechanical behavior of the human skin has been investigated. The properties of human skin have been evaluated either *in vivo* [3] or *in vitro* [2], [8]. Measurements *in vivo* allow the skin to be tested in its natural conditions, but they can be limited only to small stresses and the boundary conditions cannot be fully controlled. Tensile tests performed on excised skin samples allow the application of higher strains along varying trajectories, providing

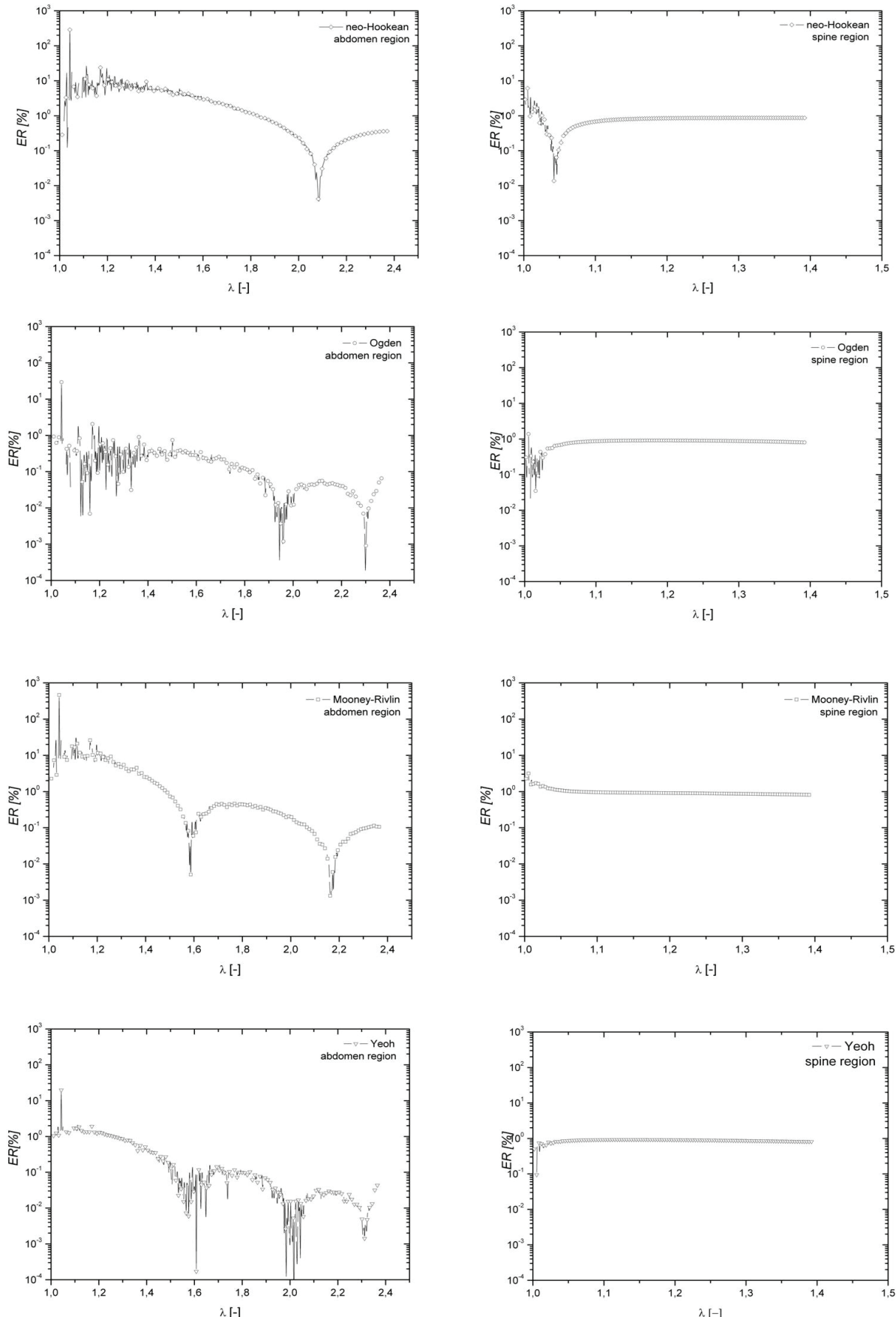


Fig. 5. The error residual between theoretical neo-Hookean, Ogden, Mooney–Rivlin, Yeoh models and the experimental data. The area of specimens taken: left – the abdomen, right – the spine

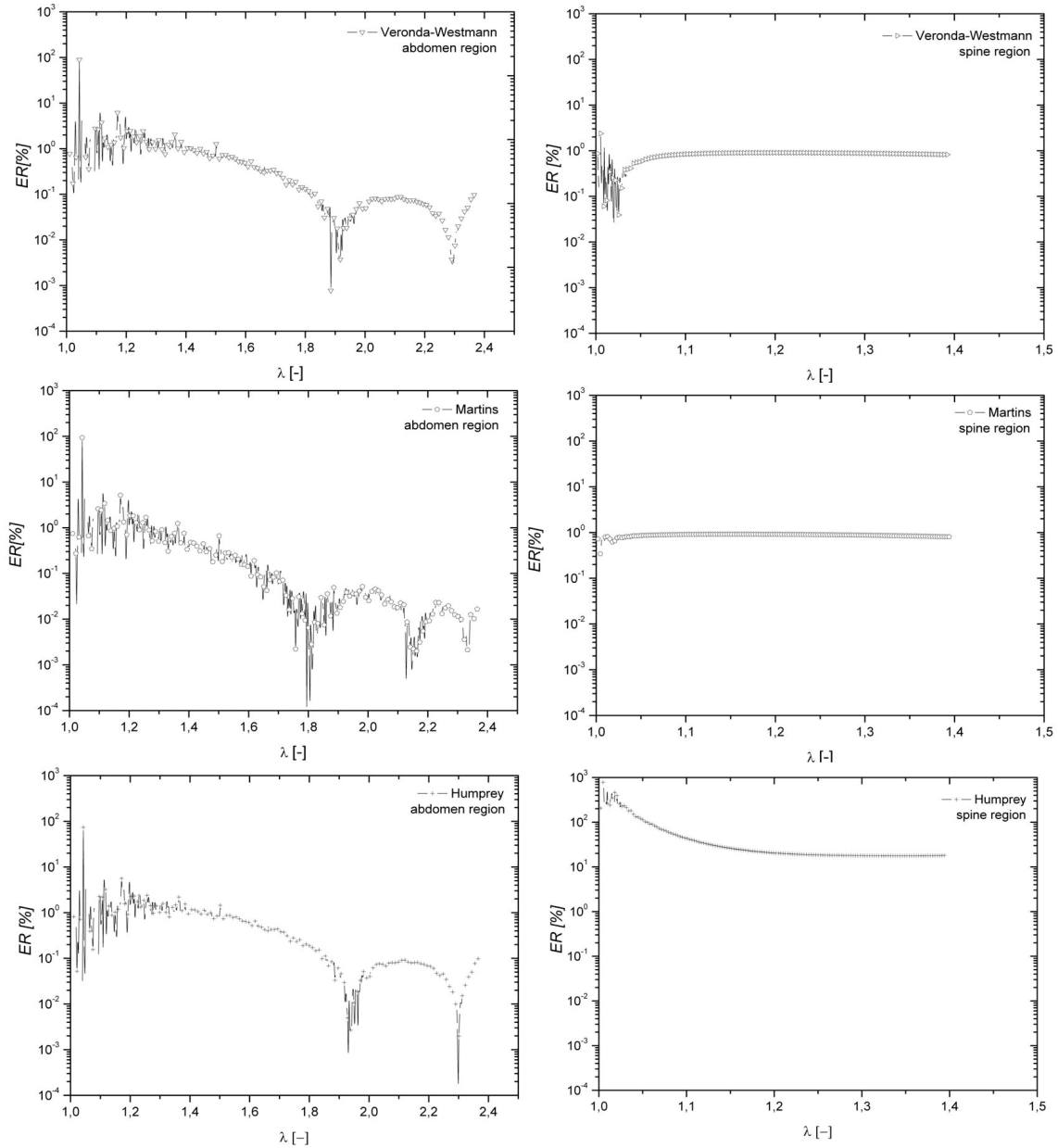


Fig. 6. The error residual between theoretical Veronda-Westman, Martins and Humphrey models and the experimental data depending on the area of skin specimens taken (left – the abdomen, right – the spine)

data about anisotropic properties related to the large levels of deformation. The shape of the stress-strain curves presented in this work was characteristic (*J*-shape) for soft biological tissues subjected to the tensile tests in both regions of the taken samples. For the presented experimental curves for two regions of the specimens taken the values of Young's modulus were calculated for two ranges of deformation matching small and large strain. For all tested group of specimens these ranges had different values. For specimens from the abdomen region it was 0 to 0.4 for the phase I and 1.0 to 1.4 for the phase III. For specimens from the spine region, it was 0 to 0.5 for the phase I and 0.13 to 0.24 for the phase III. These was

in good correspondence with results presented by Lim et al. [16]. The ultimate tensile stress in the current study was found to be in the same range as in the study made by Annaidh et al., who reported the value of UTS of 28.6 MPa for parallel human skin samples and 16.5 MPa for perpendicular human skin samples [2]. In the study of Gallagher et al. for a human skin, the mean value of ultimate tensile strength was 27.2 MPa and the value of Young's modulus was 98.9 MPa and it was similar to our results for samples taken from the back of a swine [8]. For a swine tissue, Žak et al. reported the value of the Young's modulus between 4 to 7 MPa [25], what is in agreement with our results for the abdomen region. The value of Young's modulus

of 106.8 ± 13.6 MPa, however, is higher than presented by Gąsior-Głogowska et al. [9] for the skin from the thigh of 2–12 MPa for the perpendicular and longitudinal samples respectively. The maximum stress value was 2.5 and 0.6 MPa for the samples taken along and across Langer's lines, respectively. Our results of the maximum stress were 6.09 ± 0.7 and 34.13 ± 6.27 MPa for the different region of specimens taken, the abdomen and the spine respectively. The test conditions in other studies varied greatly (difference of species, age, location, orientation, loading rate, test equipment, etc.) and no direct comparison can be made. Other studies at dynamic strain rates involved with animal skins shown the ultimate tensile stress values ranging from 0.1 to 0.3 MPa [16]. The influence of the strain rates on the stretch ratio at the ultimate stress or at failure were not termed in this study.

An analysis of the correlation between the experimental and theoretical data with the use of seven hyperelastic models showed good fitting for five models. Neo-Hookean model shown the worst performance and as the model with only one parameter was unable to capture test data for non-linear behavior of a skin tissue. Also worse matching to the experimental data was observed for two parameters of Mooney–Rivlin model for the abdomen region. The best correlation was achieved for Martins and Yeoh models, which have, respectively, four and three parameters, and it is expected to find more optimal solutions for these models. The resulting values of μ model parameter for the Ogden model in the work of Lim et al. [16] were in range of 10 to 300 kPa and 3 to 370 kPa respectively for parallel and perpendicular direction to the spine of the pig's body, and strain ratio was in the range of 0.005 to 3500 1/s, what was lower than our results. The values of strain hardening exponent was equal to 7.7 and 27.4 depending of the place of specimens taken. In the literature this parameter does not depend on strain ratio and well agrees with [16], [23]. The presence of characteristic peaks in the graphs of the error distribution curves fitting the model to experimental data matches the report of Martins et al. Similarly to this work, the worst matching was obtained for neo-Hookean model [17].

Conducted investigations considered only one chosen direction of samples taken. Due to the fact that skin tissue is a strongly anisotropic material [2], it is more appropriate to use the biaxial tensile tests. Difficulties connected with such tests make the uniaxial tensile tests for specimens taken from a skin in two directions more popular [14], [16], [23].

5. Conclusions

An analysis of seven hyperelastic material models showed good correlations between experimental and theoretical data for five models. A comparison of the match for skin specimens taken from two regions of the pig's body showed, in general, better correlations for specimens taken from the spine region. Neo-Hookean model was unable to capture non-linearity of the stress–stretch curve of skin tissue and showed the worst performance. Models with exponential formulas and with more than two parameters have better fitting to the experimental data for a swine tissue compared to polynomial models. The number of model parameters has influence on optimal solutions of the procedure of modeling of a skin tissue.

A lot of limitations associated with this study including separation of the effect of many factors such as the orientation of the fibers, places of specimens taken or anisotropy of the skin and the effect of the strain rates, requires further investigations in the future.

Acknowledgement

The work was realized due to statutory activities M-1/6/2016/DS.

References

- [1] ADULL MANAN N.F., AZIZZATI S.N., NOOR M., AZMI N.N., MAHMUD J., *Numerical investigation of Ogden and Mooney-Rivlin material parameters*, ARPN Journal of Engineering and Applied Sciences, 2015, 10(15), 6329–6335.
- [2] ANNAIDH A.N., BRUYERE K., DESTRADE M., GILCHRIST M.D., MAURINI C., OTTENIO M., SACCOMANDI G., *Automated estimation of collagen fiber dispersion in the dermis and its contribution to the anisotropic behavior of skin*, Annals of Biomedical Engineering, 2012, 40(8), 1666–1678.
- [3] BOYER G., LAQUEZE1 L., LE BOT1 A., LAQUEZE S., ZAHOUANI H., *Dynamic indentation on human skin in vivo: ageing effects*, Skin Research and Technology, 2009, 15, 55–67.
- [4] BROUWER I., USTIN J., BENTLEY L., SHERMAN A., DHARUV N., TENDICK F., *Measuring in vivo animal soft tissue properties for haptic modeling in surgical simulation*, Studies in Health Technology and Informatics, 2001, 81, 69–74.
- [5] CORR D.T., HART D.A., *Biomechanics of Scar Tissue and Uninjured Skin*, Advances in Wound Care, 2013, 2(2), 37–43.
- [6] FLATEN G.E., PALAC Z., ENGESLAND A., FILIPOVIC-GRCIC J., VANIC Z., SKALKO-BASNET N., *In vitro skin models as a tool in optimization of drug formulation*, European Journal of Pharmaceutical Sciences, 2015, 75, 10–24.
- [7] FREEMAN F., DEVORE J.D., *Viscoelastic properties of human skin and processed dermis*, Skin Research and Technology, 2001, 7, 18–23.

- [8] GALLAGHER A.J., NÍANNIADH A., BRUYERE K., OTTÉNIO M., XIE H., GILCHRIST M.D., *Dynamic Tensile Properties of Human Skin*, IRCOBI Conference, 2012, 494–502.
- [9] GAŚIÓR-GŁOGOWSKA M., KOMOROWSKA M., HANUZA J., MĄCZKA M., ZAJĄC A., PTAK M., BĘDZIŃSKI R., KOBIELARZ M., MAKSYMOWICZ K., KUROPKA P., SZOTEK S., *FT-Raman spectroscopy study of human skin subjected to uniaxial stress*, Journal of the Mechanical Behavior of Biomedical Materials, 2013, 18, 240–252.
- [10] HOLZAPFEL G.A., *Biomechanics of Soft Tissue*, Computational Biomechanics, Biomech preprint series, 2000.
- [11] JOR J.W.Y., NASH M. P., NIELSEN P.M.F., HUNTER P.J., *Estimating material parameters of a structurally based constitutive relation for skin mechanics*, Biomechanics and Modeling Mechanobiology, 2011, 10, 767–778.
- [12] KARIMI A., RAHMATIC S.M., NAVIDBAKHSH M., *Mechanical characterization of the rat and mice skin tissues using histosstructural and uniaxial data*, Bioengineered, 2015, 6(3), 153–160.
- [13] KUMAR S., LIU G., SCHLOERB D., SRINIVASAN M.A., *Viscoelastic characterization of the primate finger pad in vivo by micro step indentation and three-dimensional finite element models for tactile sensation studies*, Journal of Biomechanical Engineering, 2015, 137, 1–10.
- [14] ŁAGAN S., LIBER-KNEĆ A., *A characteristic of anisotropic mechanical properties of a pig's skin*, Engineering of Biomaterials, 2014, 17(128–129), 61–63.
- [15] LATORRE M., MONTÀNS F.J., *On the tension-compression switch of the Gasser–Ogden–Holzapfel model: Analysis and a new pre-integrated proposal*, Journal of the Mechanical Behavior of Biomedical Materials, 2016, 57, 175–189.
- [16] LIM J., HONG J., CHEN W.W., WEERASOORIYA T., *Mechanical response of pig skin under dynamic tensile loading*, International Journal of Impact Engineering, 2011, 38, 130–135.
- [17] MARTINS P.A.L.S., NATAL JORGE R.M., FERREIRA A.J.M., *A comparative study of several material models for prediction of hyperelastic properties: Application to silicone-rubber and soft tissues*, Strain, 2006, 42, 135–147.
- [18] MOERMAN K.M., SIMMS C.K., NAGEL T., *Control of tension–compression asymmetry in Ogden hyperelasticity with application to soft tissue modeling*, Journal of the Mechanical Behavior of Biomedical Materials, 2016, 56, 218–228.
- [19] MORIERA P., MISRA S., *Biomechanics-based curvature estimation for ultrasound-guided flexible needle steering in biological tissues*, Annals of Biomedical Engineering, 2015, 43(8), 1716–1726.
- [20] NESBITT S., SCOTT W., MACIONE J., KOTHA S., *Collagen fibrils in skin orient in the direction of applied uniaxial load in proportion to stress while exhibiting differential strains around hair follicles*, Materials, 2015, 8, 1841–1857.
- [21] OGDEN R.W., SACCOMANDI G., SGURA I., *Fitting hyperelastic models to experimental data*, Computational Mechanics, Springer-Verlag, 2004, 34, 484–502.
- [22] STARK M.M., *Clinical forensic medicine: a physician's guide*, Humana Press, 2005.
- [23] SHERGOLD O.A., FLECK N.A., RADFORD D., *The uniaxial stress versus strain response of pig skin and silicone rubber at low and high strain rates*, International Journal of Impact Engineering, 2006, 32, 1384–1402.
- [24] TEPOLE A.B., GOSAIN A.K., KUHL E., *Computational modeling of skin: Using stress profiles as predictor for tissue necrosis in reconstructive surgery*, Computers and Structures, 2014, 143, 32–39.
- [25] ŹAK M., KUROPKA P., KOBIELARZ M., DUDEK A., KALETAKURATEWICZ K., SZOTEK S., *Determination of the mechanical properties of the skin of pig fetuses with respect to its structure*, Acta of Bioengineering and Biomechanics, 2011, 13(2), 37–43.